Double-pass imaging polarimetry in the human eye

Juan M. Bueno and Pablo Artal

Laboratorio de Optica, Departamento de Física, Universidad de Murcia, Campus de Espinardo (Edificio C), 30071 Murcia, Spain

Received September 9, 1998

A Mueller-matrix imaging polarimeter was developed to measure spatially resolved polarization properties in the living human eye. The apparatus is a double-pass setup that incorporates two liquid-crystal variable retarders and a slow-scan CCD camera in the recording stage. Series of 16 images for the combinations of independent polarization states in the first and second passages were recorded for two experimental conditions: with the camera conjugated either with the retina or with the eye's pupil plane. Spatially resolved collections of Mueller matrices and the degree of polarization were calculated from those images for both retinal and pupil planes. © 1999 Optical Society of America

OCIS codes: 120.5410, 170.3880, 330.5370.

Because the ocular media and the retina in the human eye exhibit rather complicated polarization properties, every technique based on collecting the light scattered back into the retina, for instance, the retinal image quality measured by use of either the double-pass method[1,2] or the Hartmann–Shack sensor,[3,4] is affected by polarization. On the other hand, several diagnostic techniques currently used in ophthalmology are based on measuring changes in the polarization state in the retina.[5] Earlier experiments used only parallel and crossed linear polarizers,[6,7] and van Blokland[8] used a rotating retarder polarimeter to measure the polarization properties of the light backscattered from the retina. Dreher *et al.*[5] developed a Fourier ellipsometer adapted to a laser scanning ophthalmoscope for clinical applications. A confocal imaging electro-optical ellipsometer has been used to measure the birefringence of the living retina.[9] Polarimeters that used Fourier analysis of a single detected signal found many applications[10,11] in addition to purely ophthalmic ones. An imaging polarimeter that uses a CCD camera and dual rotating retarders was also reported recently.[12] Here we present an imaging polarimeter without mobile parts, which uses liquid-crystal variable retarders (LCVR's) adapted to an ophthalmoscopic double pass (D-P) apparatus. It allows spatially resolved Mueller matrices (MM's) in the living human eye to be measured at both the pupil and the retinal planes.

The apparatus (Fig. 1) is a D-P configuration[1,2] incorporating two electronically controlled LCVR's, one in the first pass [polarization-state generator (PSG)] and the other in the second pass [polarization-state analyzer (PSA)]. To calculate the 16 elements of the MM requires at least 16 measurements for independent polarization states of PSG–PSA combinations.[13] Driving the LCVR's with appropriate voltages (defined after calibration) can produce only three completely independent states of polarization. These states are approximately linear horizontal, linear vertical, and right circular. Placing two additional quarter-wave plates in the entrance and exit optical paths produces a fourth state (approximately 45° linear). The eye is illuminated by a 633-nm He–Ne laser beam, an afocal system (lenses L_2 and L_3) allows the beam to be focused correctly on the retina, and a scientific-grade slow-scan CCD camera records images of either the retina or the eye's pupil plane, depending on the placement of lens L_4. Red light was used to reduce bleaching of the photoreceptors, which could affect the polarization of backscattered light.[14] Reference intensities recorded by a photodiode were used to correct the mean intensity level in the images, according to fluctuations of the light source. First we calibrated the complete setup to determine the accuracy of the instrument. The identity matrix of the air was measured with errors of less than 0.5% in each coefficient. A quarter-wave plate was also

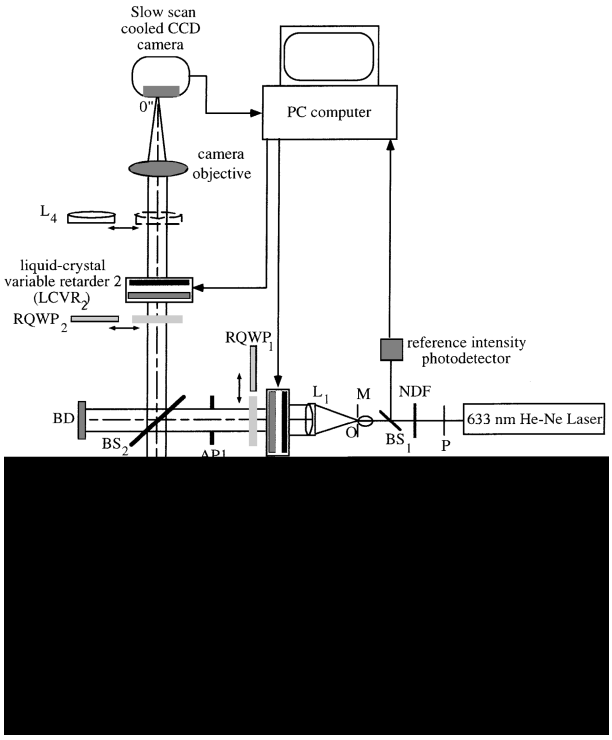

Fig. 1. Schematic diagram of the imaging polarimeter: P, linear polarizer; NDF, neutral-density filter; O, point source; BS_1, pellicle beam splitter to measure the reference intensity with the detector; M, microscope objective; $RQWP_1$, $RQWP_2$, removable quarter-wave plates; BS_2, pellicle beam splitter; L_1–L_4, achromatic lenses; AP_1, AP_2, apertures acting as the stop for the first and second passes, respectively; BD, light trapper; O′, retinal image; O″, D-P image.

0146-9592/99/010064-03$15.00/0

measured with the apparatus for three orientations of the fast axis. The measured values of retardation (180° expected) and azimuth[15] were $(178.2, -0.5)$, $(179.9, 30.6)$, and $(179.4, 44.4)$ for 0°, 30°, and 45° orientation, respectively.

Series of 16 images (4-s exposure time and 256×256 pixels with 16 bits/pixel) were recorded for the combinations of polarization states in the incoming and outgoing paths. The series of images corresponds either to D-P retinal images of a point source (with 2- and 5-mm pupil diameters) or to pupil plane images (illuminating the eye with a 2-mm-diameter beam). Noise in the images was reduced by application of a median filter. Every D-P retinal image was subsampled to 32×32 pixels (each pixel corresponded to 0.92 min of arc of visual field). The corneal reflex, which appeared quite bright and localized in the images of the pupil, was digitally removed, and those images were also subsampled to 48×48 pixels (with each pixel corresponding to 0.16 mm). The MM's of the eye plus the retina were calculated for each pixel of the images by a matrix inversion method briefly described in what follows.

For each polarization state produced by the PSG [with a Stokes vector $S_{\mathrm{PSG}}^{(m)}$], the light emerging from the PSA, before it reaches the CCD camera, has a Stokes vector $[S_{\mathrm{PSA}}^{(n)}]$ given by

$$S_{\mathrm{PSA}}^{(n)} = \overline{M}_{\mathrm{PSA}}^{(n)} M_T M M_R S_{\mathrm{PSG}}^{(m)}, \tag{1}$$

where M_T and M_R are the MM's of the pellicle beam splitter (BS_2 in Fig. 1) in transmission and reflection, respectively, previously measured in the calibration process; M is the MM of the eye, including the two passes, and $\overline{M}_{\mathrm{PSA}}^{(n)}$ is one of the four MM's of the PSA (each corresponding to an independent state). For every $S_{\mathrm{PSG}}^{(m)}$ there are four $\overline{M}_{\mathrm{PSA}}^{(n)}$, four Stokes vectors $S_{\mathrm{PSA}}^{(n)}$, and four intensities (pixel values in each image) I_{mn} $(n = 1, 2, 3, 4)$. Because four independent $S_{\mathrm{PSG}}^{(m)}$ $(m = 1, 2, 3, 4)$ are considered, sixteen values of intensity (I_{mn}) are recorded. Let M_{PSA} be an auxiliary 4×4 matrix, with each row being the first row of every $\overline{M}_{\mathrm{PSA}}^{(n)}$, $S_{\mathrm{OUT}}^{(m)}$ be the Stokes vector that corresponds to every state coming back from the eye and before it enters the PSA when $S_{\mathrm{PSG}}^{(m)}$ is produced by the PSG $[S_{\mathrm{OUT}}^{(m)} = M_T M M_R S_{\mathrm{PSG}}^{(m)}]$, and $M_{S\text{-OUT}} = [S_{\mathrm{OUT}}^{(1)}, S_{\mathrm{OUT}}^{(2)}, S_{\mathrm{OUT}}^{(3)}, S_{\mathrm{OUT}}^{(4)}]$ be an auxiliary matrix. Then

$$I_{mn} = M_{\mathrm{PSA}} M_{S\text{-OUT}}, \tag{2}$$

where I_{mn} is another auxiliary 4×4 matrix whose elements are the intensity measurements for the 16 combinations of the PSG–PSA. By inversion of Eq. (2) the elements of $M_{S\text{-OUT}}$ are obtained. Finally, the MM of the eye (M) is computed by

$$M = (M_T)^{-1} M_{S\text{-OUT}} (M_{\mathrm{PSG}})^{-1} (M_R)^{-1}, \tag{3}$$

where $M_{\mathrm{PSG}} = [S_{\mathrm{PSG}}^{(1)}, S_{\mathrm{PSG}}^{(2)}, S_{\mathrm{PSG}}^{(3)}, S_{\mathrm{PSG}}^{(4)}]$ is the auxiliary 4×4 matrix whose columns are the four Stokes vectors of the states produced by the PSG. By this procedure a MM is obtained at each pixel of the images. These results are conceptually similar to the polarization-aberration functions and point-spread matrices previously reported for general optical systems,[12,16] although in this case the matrices contain information on the two passages through the eye and the retinal reflection.

Spatially resolved MM's were measured in three normal subjects for the D-P retinal image in the fovea and the eye's pupil plane. As an example, results for one of the subjects are presented. Figure 2 shows the D-P MM retinal images obtained with a 2-mm pupil diameter. Each image corresponds to one element of

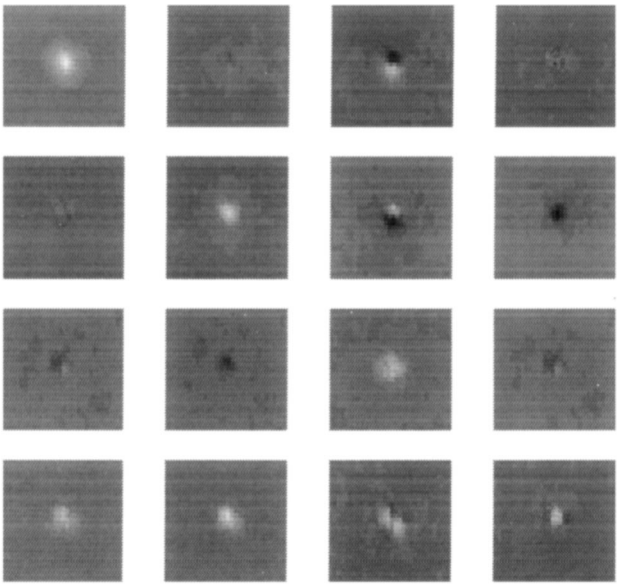

Fig. 2. Images corresponding to the elements of the D-P MM's in the eye. The elements in the top row are 1-1, 1-2, 1-3, and 1-4 from left to right. Each image subtends 29 min of arc of visual field. The gray level code is the following: white is 1, black is −1, and gray is zero.

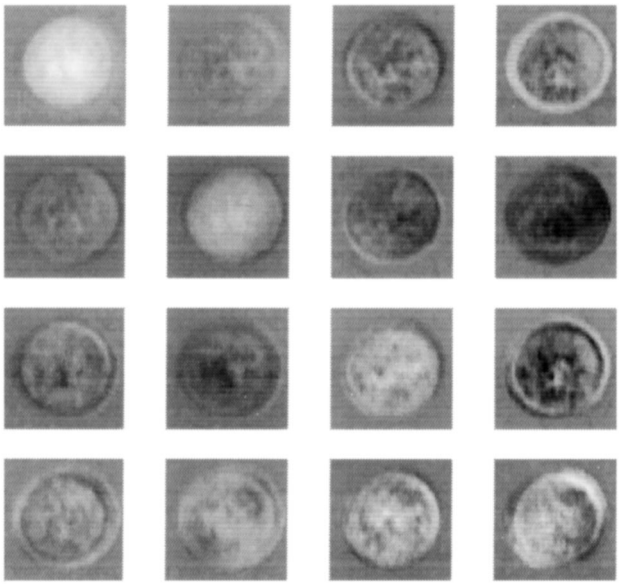

Fig. 3. Images corresponding to the elements of the eye's pupil plane MM's in the eye. Each image corresponds to 7.7 mm in the pupil plane. The gray level code is the same as for Fig. 2.

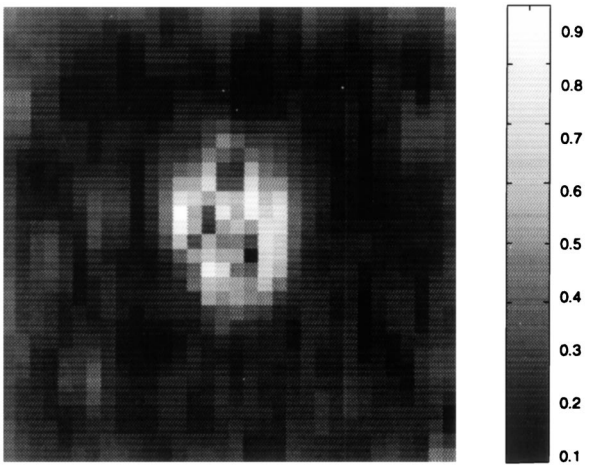

Fig. 4. Degree of polarization in the D-P image (obtained with a 2-mm pupil diameter). The image subtends 29 min of arc of visual field. The gray code ranges from white (0.9) to black (0.1).

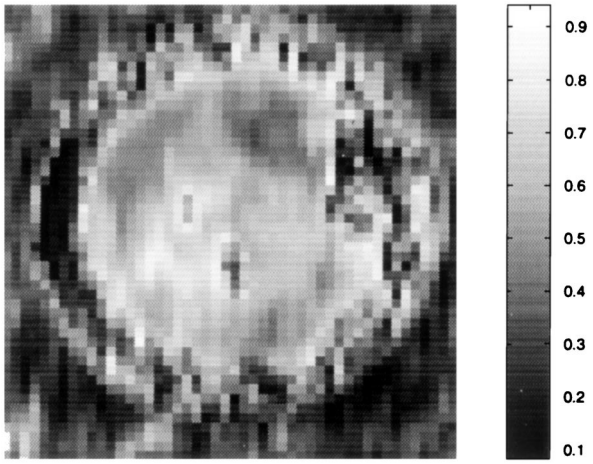

Fig. 5. Degree of polarization in the eye's pupil plane. The image subtends 7.7 mm over the pupil. The gray code ranges from white (0.9) to black (0.1).

the matrix and subtends 29 min of arc. The matrix elements are normalized to the maximum of element (1-1). Figure 3 shows the MM in the pupil plane for the same subject. Every image represents a value of the elements of the MM over the eye pupil and has a full size of 7.7 mm. From the results of Fig. 2 and by simple matrix calculations, D-P images of a point source and their corresponding modulation transfer functions[2] for light incident to the eye with different polarization states are obtained. This process is a powerful tool for predicting the polarization-related aberrations in the human eye and the retina. By direct inspection of Fig. 2 it is easy to note that, because the images of matrix elements (1-2) (1-3), and (1-4) are not constant, the D-P images for light with linear horizontal and vertical polarization, ±45° linear and right and left circular, respectively, are not exactly the same. This result indicates that the D-P method yields slightly different results for the eye's optical performance, depending on the polarization state of the incident light.

A further analysis of the MM was also performed to extract a spatially resolved degree of polarization.[17] This parameter is the percentage of the incident light that remains polarized, although it can be in a different polarization state, after a double pass through the eye media and reflection in the retina. Figures 4 and 5 shows the degrees of polarization that correspond to the D-P images and to the eye's pupil plane, respectively. These results confirm earlier experiments with parallel and crossed linear polarizers,[18] suggesting that most of the light that forms the central parts of the D-P images remains polarized, while the skirt contains depolarized light. Our results show that, for 2-mm pupil diameter, ~80% of the light that forms the cores of the D-P images remains polarized, whereas in the skirt (from ~12 min of arc off center) only 20% of the light is polarized. The degree of polarization follows approximately the shape of the intensity in the retinal image. For the 5-mm pupil diameter, the percentage of polarized light that forms the core of the image is lower.

In conclusion, we have developed an imaging polarimeter to be used in the living eye and have presented series of spatially resolved MM's for the retinal and pupil planes. The instrument could be adapted to record high-magnification polarization-coded images of the retina or be used with minor modifications in other applications.

This research was supported by Dirección General de Investigación Científica y Técnica (Spain) grants PB94-1138 and HA96-0022. The authors thank J. J. Gil, B. Pelz, and S. Goelz for their comments. P. Artal's e-mail address is pablo@fcu.um.es.

References

1. J. Santamaría, P. Artal, and J. Bescós, J. Opt. Soc. Am. A **4,** 1109 (1987).
2. P. Artal, I. Iglesias, N. López-Gil, and D. G. Green, J. Opt. Soc. Am. A **12,** 2358 (1995).
3. J. Liang, B. Grimm, S. Goelz, and J. F. Bille, J. Opt. Soc. Am. A **11,** 1949 (1994).
4. J. Liang and D. R. Williams, J. Opt. Soc. Am. A **14,** 2873 (1997).
5. A. W. Dreher, K. Reiter, and R. N. Weinred, Appl. Opt. **31,** 3730 (1992).
6. R. A. Weale, J. Physiol (London) **186,** 9325 (1966).
7. W. N. Charman, Br. J. Physiol. Opt. **34,** 34 (1980).
8. G. J. van Blokland, J. Opt. Soc. Am. A **2,** 72 (1985).
9. B. Pelz, C. Weschenmoser, S. Goelz, J. P. Fisher, O. W. Burk, and J. Bille, Proc. SPIE **2930,** 92 (1996).
10. R. A. Chipman, in *Handbook of Optics*, 2nd ed., M. Bass, ed. (McGraw-Hill, New York, 1995), Sec. 22.1.
11. R. M. A. Azzam, in *Handbook of Optics*, 2nd ed., M. Bass, ed. (McGraw-Hill, New York, 1995), Sec. 27.1.
12. J. L. Pezzaniti and R. A. Chipman, Opt. Eng. **34,** 1558 (1995).
13. P. S. Hauge, J. Opt. Soc. Am. **68,** 1519 (1978).
14. G. J. van Blokland and D. van Norren, Vision Res. **26,** 485 (1986).
15. J. J. Gil and E. Bernabeu, Optik **76,** 67 (1987).
16. J. P. McGuire and R. A. Chipman, J. Opt. Soc. Am. A **7,** 1614 (1990).
17. J. J. Gil and E. Bernabeu, Opt. Acta **33,** 185 (1985).
18. R. Rohler, U. Miller, and M. Aberl, Vision Res. **9,** 407 (1969).